Repetitive control for radial tracking of a CD-player

Report of traineeship:

Repetitive control for radial tracking of a CD-player

By: J.J.M.v.d.Wijdeven
DCT 2001-67

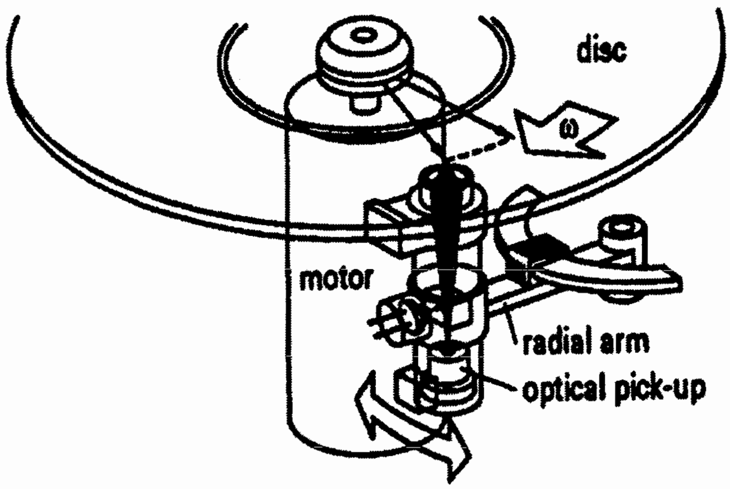

21-12-2001

Supervised by:
Prof. Dr. Ir. M. Steinbuch

Contents

Introduction

In the past compact disks have mainly been used for audio appliances. Nowadays, the number of applications for optical storage devices is growing rapidly. Through time, the CD can contain more and more data while the size of the disk remains unchanged or gets even smaller. This has as result that the tracking error of an optical storage device must decrease in order to have a proper functioning optical storage device.
In the future, the specifications for tracking errors for optical storage devices will get more demanding. Some of the applications where the tracking error must be reduced are the CD-rom and the DVD. The normal feedback controller may not be sufficient enough to keep the radial arm of the reading mechanism inside the specified boundaries.

The influence of the periodic errors from the eccentricity of the tracks and the disk and wobbling of the spindle motor on the total error is relatively large. So, if one can find a controller that can deal with those periodic disturbances, the total error can be greatly reduced.
A controller that can filter out periodic disturbances from the error signal is the repetitive controller. Besides that control algorithm, two robust versions of repetitive control will be introduced. With the robust repetitive controller uncertainties in the period time should have less influence on the tracking error than the normal repetitive controller.

The goal of this report is: 'The research and implementation of repetitive and robust repetitive control for radial tracking of a CD-player'.
This will be done by first investigating the experimental CD-set-up and finding a feedback controller that meets the specifications (chapter 2). After that the theory behind repetitive and robust repetitive control will be discussed (chapter 3). With that knowledge the repetitive controllers will be designed and the problems that occur are dealt with (chapter 4).
First the repetitive and robust repetitive controllers will be tested via simulation in Simulink (chapter 5) after which experiments with the CD-set-up shall be done (chapter 6). This report ends with the conclusions and recommendations for further research.

2. Modelling and feedback control

The repetitive control idea is based on the internal model principle. This means that one can see the repetitive controller as an add-on part to a normal feedback model and that it includes a model of the external disturbances.
Before the repetitive controller can be implemented, there has to be a model of the CD-player and a simple feedback controller. This will be done in two phases. In the first phase a feedback controller will be designed for the nominal plant. In the second phase, the plant will be extended with the dynamics of the digital implementation device, after which the final feedback controller will be designed.

2.1 Phase one

In this study the radial transfer function of the CD-player (plant, *P*) is obtained by measuring the sensitivity (*S*) of the experimental set-up. Before the plant can be subtracted from the sensitivity, the internal (print board) PID controller (*C*) is measured. For more details on the measurements on de CD-set-up, see the reports [1-3]

With the use of formula 2.1 the transfer function of the plant has been found. In figure 2.1 the plant is shown.

$$P = \frac{S^{-1} - 1}{C} \qquad 2.1$$

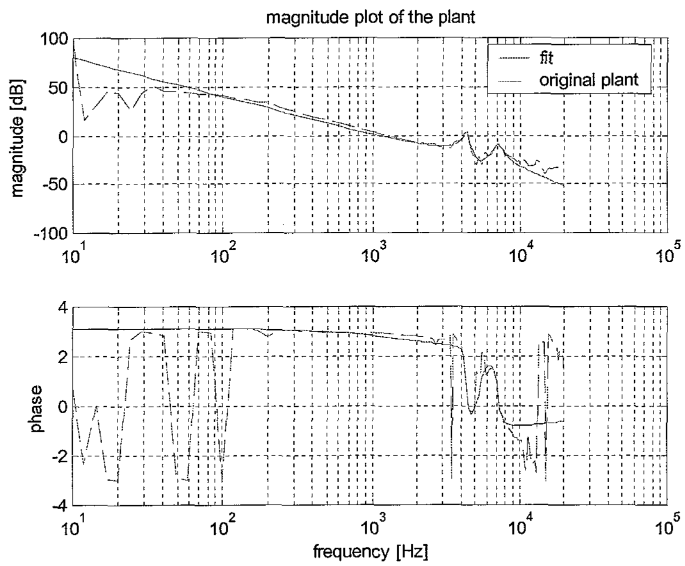

Figure 2.1, Bode plot of the measured plant and its fit

The smooth line in figure 2.1 is an eight-order fit of the plant. With this fit a controller is build, so that the open loop system has a bandwidth of approximately 700 Hz, the maximum absolute sensitivity is under the 6 dB and the phase margin is at least 35 degrees.
Besides those specifications the sensitivity value at the rotation frequency (around 12 Hz) must be less than –60 dB to reach the demands of the manufacturer. The reason for this is because the CD's are made with a track accuracy of 100 μm while the maximum allowed radial tracking error is 0.1 μm.

The final controller is shown in figure 2.2 and has two lead lags and a notch at the first resonance of the plant.

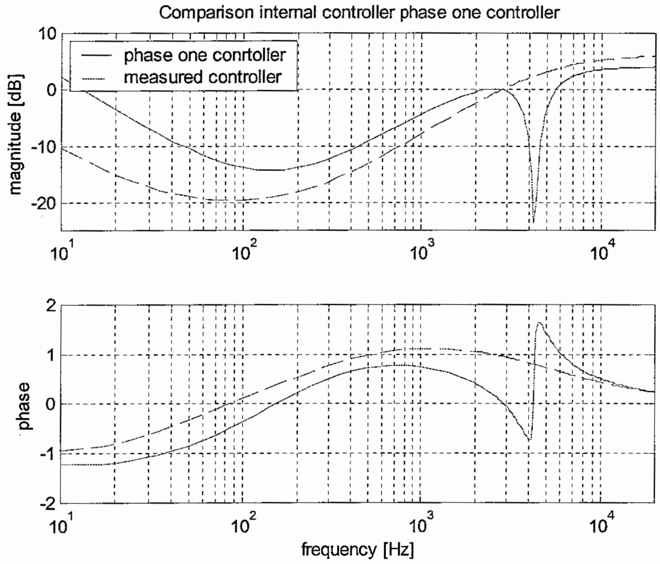

Figure 2.2, comparison between the measured controller and the phase one controller

2.2 Phase two

Further on in the study, experiments with the designed controllers will be done. This is possible with the use of a Dspace instrument that can implement the controllers in real time. Dspace has some dynamics and it needs time to convert signals from analogue to digital and back. The last issue will result in a time delay in the system.

One can account for the dynamics of Dspace, by putting it in the model of the plant and consider the combination as the new model for the plant. For the new plant model a new controller can be designed. This way, the dynamics of Dspace are accounted for and it won't have any effect on the total model of the CD-set-up anymore.

In figure 2.3 and 2.4 respectively the new plant model and controllers are shown.

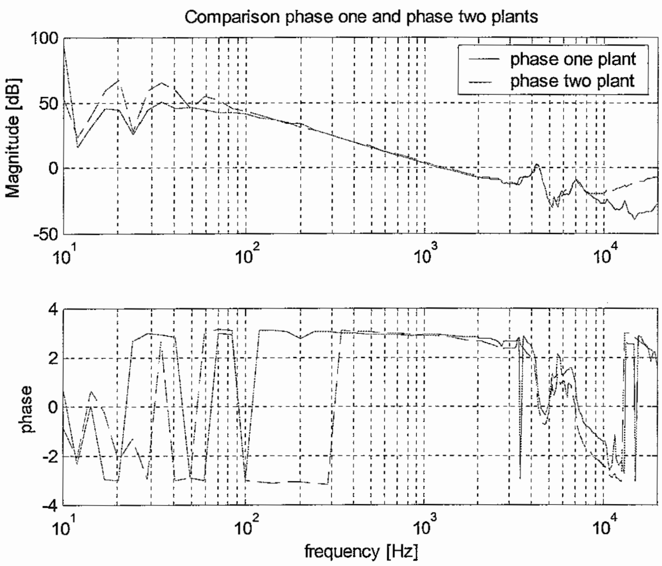

Figure 2.3, comparison between the Bode plots of the phase one and phase two plants

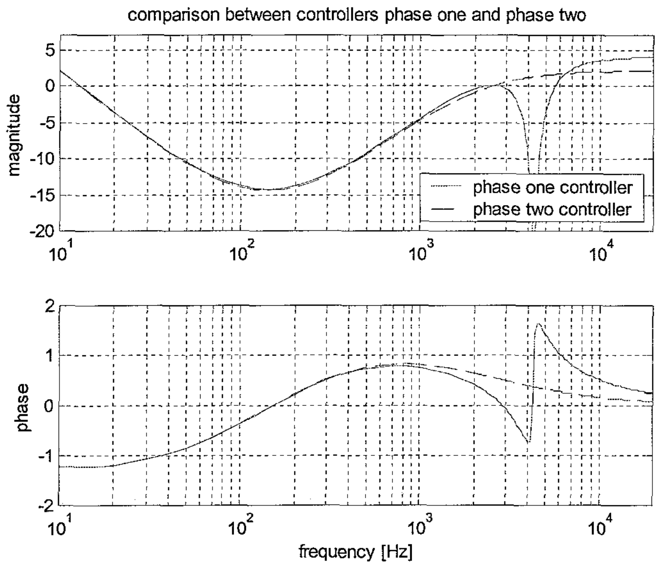

Figure 2.4, comparison phase one and phase two controller

One can see that the new plant has a delay: the phase falls off at higher frequencies. At 10 kHz, the phase shift is around 1 rad/s. With a sample frequency of 36 kHz, the delay is 0.55 samples. 0.5 samples is the result of the ZOH of the discrete time implementation of the model; 0.05 samples is the result of conversions.

With respect to stability, a notch is not needed in the plant of phase two. Looking back to the controller of phase one the notch isn't necessary either. However, the presence of the notch in phase one does not give any problems for the continuation of this study and thus the phase one controller isn't adapted.

With the found controllers simulations have been done. The reference signal is a combination of the rotation frequency and the first two harmonics. The maximum amplitude of the reference signal is approximately 100 μm. In figure 2.5 the error signals are plotted.

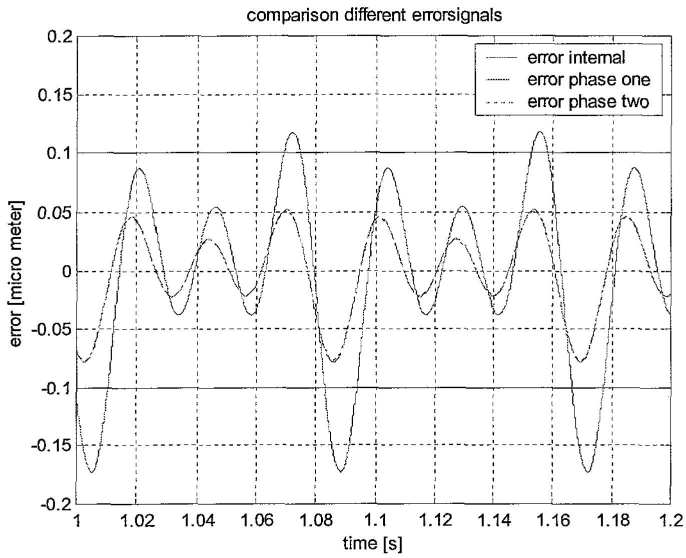

Figure 2.5, comparison error signals generated by the different controllers

As can be seen, the internal controller does not meet the requirements. The phase one and phase two controllers have the same error signal (the two lines lay over each other) and do meet the requirements. The reason why the error signals are asymmetric is because the phase of the reference signal has effect on the steady state errors.
Finally experiments with the controllers have been done on the CD-set-up by implementing the different controllers in Dspace. In figure 2.6 the results are presented.
The results are given by the cumulative power spectra. This is done to show the influence of the different frequencies in the error signal on the total error signal. The maximum values can be compared with each other and give an idea about the amplitude ratios between the different error signals. The absolute final value of a single cumulative power spectrum is of little use, because its value depends on the parameters that are used to calculate the spectrum.

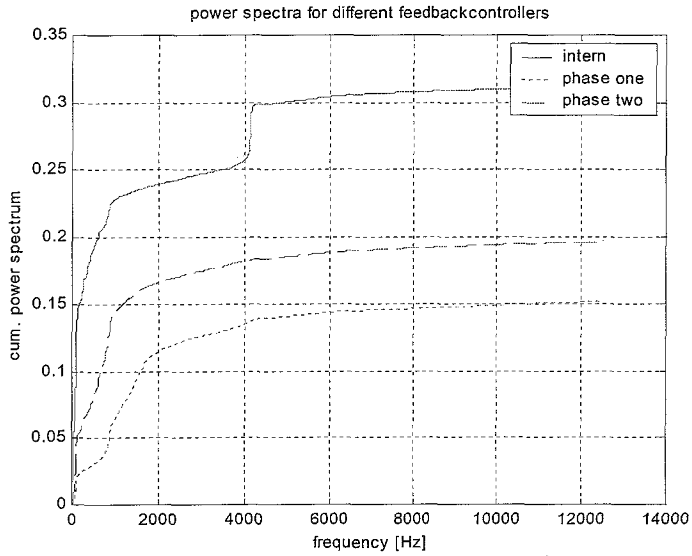

Figure 2.6, cumulative power spectrum of the three feedback controllers

The internal controller gives the largest maximum cumulative power value. One can see the influence of the first resonance of the CD-player (4000 Hz) on the tracking error. The phase one controller gives the best results. The expectation is that the phase one and two controllers give approximately the same power spectra, since the dynamics of Dspace has been accounted for by the phase two controller. The reason why the difference in the magnitude of the errors is so large is not known. Perhaps there have occurred some measurement-errors during the experiments that have not been noticed.
Nonetheless, the rest of this study makes use of the phase two controller.

3. Theory behind (robust) repetitive control

Repetitive control makes use of memory loops. If one wants to understand repetitive control, the dynamics of memory loops must be understood first. In this chapter the dynamics of a memory loop will be investigated and the influence of memory loops on the dynamics of the whole CD-model will be looked at. Of course stability of the system is very important. The stability of a closed loop system with repetitive control will be investigated by using the small gain theorem. Consequences of this theorem will be discussed. Finally two robust versions of repetitive control will be explained and stability of the two will be investigated.

3.1 Memory loops

A memory loop is a loop that exists of a delay and a positive feedback loop. In figure 3.1 scheme of the loop is shown.

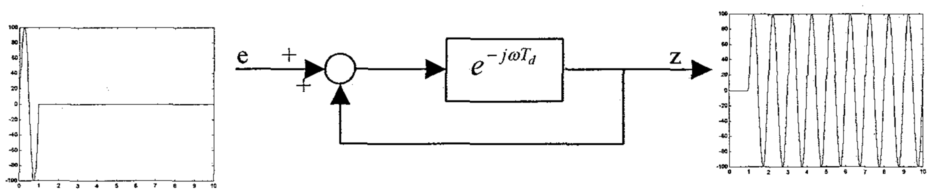

Figure 3.1, memory loop configuration

As can be seen, if one single period of a sine is given as an input, the output will generate a continuous sine with one period delay. The delay time should be the time of one period. In case of the CD-player set-up, the period time equals the time of one cycle of the disk or the inverse of the rotation frequency.
In terms of frequency responses, a delay in continuous time representation is given by formula 3.1

$$delay(j\omega) = e^{-j\omega T_d} \qquad 3.1$$

with ω the frequency [*rad/s*] and T_d the delay time or period time [*s*]. The amplitude of the delay always equals one, the phase shift equals $-\omega T_d$. If the delay would be plotted in complex plane, it would be the unity circle.
The frequency response of the memory loop has the following form:

$$M(j\omega) = \frac{e^{-j\omega T_d}}{1 - e^{-j\omega T_d}} \qquad 3.2$$

If the delay equals 1+0j, M goes to infinity. This is the case for $\omega = k2\pi/T_d$, $k = 0, 1, 2, 3, \ldots$ The magnitude plot for the memory loop is given in figure 3.2.

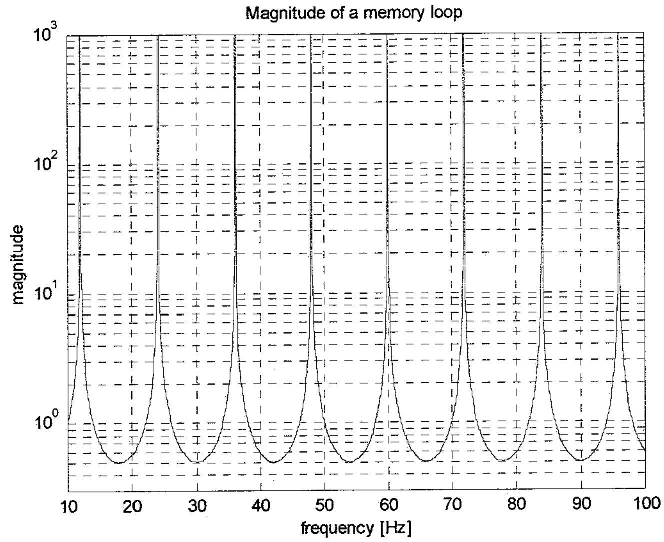

Figure 3.2, magnitude plot of a basic memory loop

As can be seen, at the rotation frequency and its harmonics the amplitude goes to infinity.

3.2 Repetitive control

Repetitive control uses the fact that a memory loop gives infinite gain at the rotation frequency and its harmonics. When the memory loop is added to a normal feedback model in a way as shown in figure 3.3, the basic repetitive control configuration is formed [4].

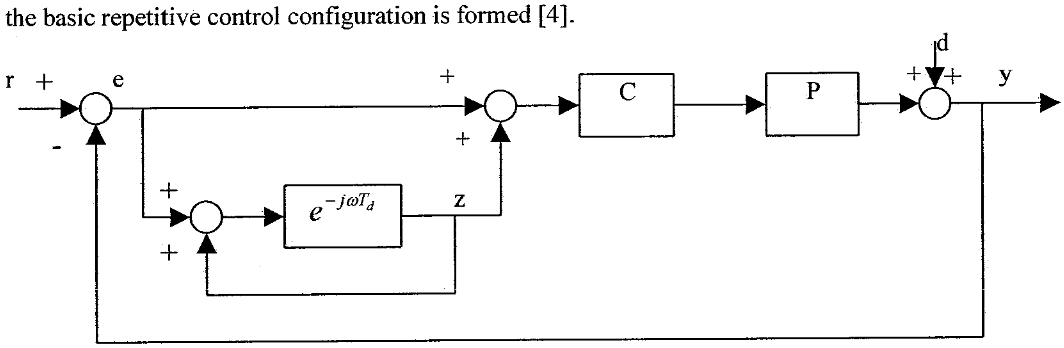

Figure 3.3, basic repetitive control configuration

The sensitivity function of this scheme is given by formula 3.3. The sensitivity function is of great importance in this study because this function gives the relation between the disturbances d and the tracking error e.

$$S(j\omega) = \frac{e}{d} = \frac{-1}{1+PC(1+M)} = \frac{-1}{1+PC(1+\frac{e^{-j\omega T_d}}{1-e^{-j\omega T_d}})} \qquad 3.3$$

If there is no memory loop, M is zero and the standard sensitivity function appears again.
Looking at the sensitivity, when M goes to infinity (at $\omega = k2\pi/T_d$), S goes to zero. In this way, the disturbances at those frequencies will be suppressed (almost) completely. The frequencies of the main

disturbances (the eccentricity of the disk and tracks and the wobbling of the spindle motor) are at $\omega = k2\pi/T_d$ and thus reduced dramatically.
In figure 3.4 the sensitivity described by formula 3.3 is plotted.

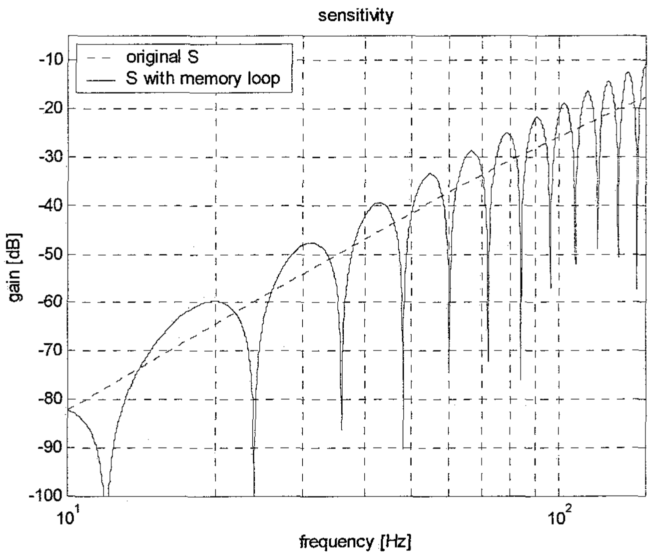

Figure 3.4, magnitude of the sensitivity function

As expected, at the periodic frequencies S becomes very small (due to numerical causes, the peeks do not go to zero). But what's also important is that between the period frequencies the sensitivity is doubled (+6 dB). This means that the errors at frequencies between the period frequencies will be two times as large with the repetitive controller than without the repetitive controller.

3.3 Stability

Before repetitive control can be used the stability of the repetitive control configuration must be investigated. To be able to look at the stability of the sensitivity function, S has to be written as given in formula 3.4c [4]. This is done by following the next steps:

$$S(j\omega) = \frac{-1}{1+PC+PC\dfrac{e^{-j\omega T_d}}{1-e^{-j\omega T_d}}} = \frac{-(1-e^{-j\omega T_d})}{(1+PC)(1-e^{-j\omega T_d})+PCe^{-j\omega T_d}} \qquad 3.4a$$

$$= \frac{-1}{1+PC}\cdot\left[\frac{1-e^{-j\omega T_d}}{1-e^{-j\omega T_d}+\dfrac{PC}{1+PC}e^{-j\omega T_d}}\right] = \frac{-1}{1+PC}\cdot(1-e^{-j\omega T_d})\cdot\left[\frac{1}{1-e^{-j\omega T_d}(1-\dfrac{PC}{1+PC})}\right] \qquad 3.4b$$

$$S(j\omega) = \frac{-1}{1+PC}\cdot(1-e^{-j\omega T_d})\cdot\left[\frac{1}{1-e^{-j\omega T_d}(1-T)}\right], \qquad T = \frac{PC}{1+PC} \qquad 3.4c$$

Between the brackets in the expression for S, there appears a fraction. This fraction is equal to the transfer function of a positive feedback loop. In a scheme, the sensitivity will look as in figure 3.5.

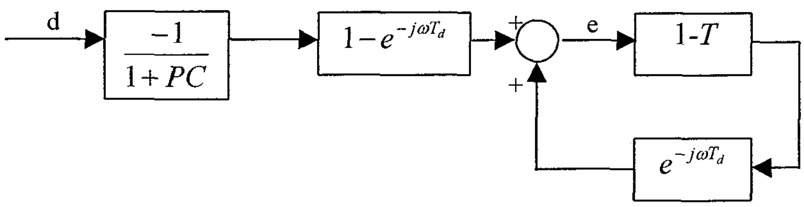

Figure 3.5, small gain theorem

To guarantee asymptotic stability a sufficient but not necessary condition is that the feedback loop should have a gain that's smaller than 1. The former is better known as the small gain theorem.
Looking at the feedback loop the stability criterion is equal to $|1\text{-}T| < 1$. Generally this statement is not guaranteed, because

$$\max|1-T| = \max|S| > 1 \qquad 3.5$$

A possible solution to stabilize the stability condition is to add a learning filter L. The memory loop now gets the configuration shown in figure 3.6.

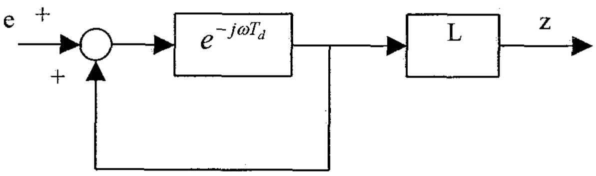

Figure 3.6, memory loop configuration with learning filter L

The stability condition becomes:

$$|1-LT| < 1 \qquad 3.5b$$

For $L = kT^{-1}$, where k is the learning gain (0 < k < 2), stability is guaranteed. (Often the inverse complementary sensitivity is unstable. In the next chapter the precise filters will be derived. For now it's sufficient to know that the learning filter should look like T^{-1}.)
For high frequencies the modelling usually is uncertain. Noise will have a great influence on the frequency response at those frequencies. With the possibility that the modelling is uncertain, one cannot guarantee that the stability condition is still met, since T is uncertain. To avoid this problem, a low pass filter Q is introduced. In this way, the memory loop will give only a small signal for high frequencies. The criterion now becomes:

$$|Q(1-LT)| < 1 \qquad 3.5c$$

The final repetitive scheme becomes:

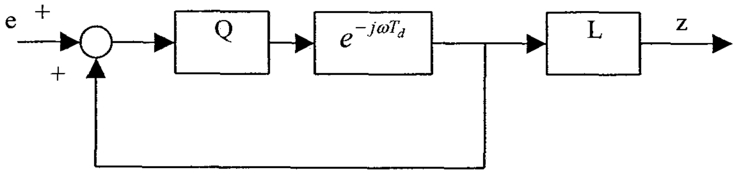

Figure 3.7, Final memory loop configuration

The frequency response of the final memory loop is given by formula 3.6.

$$M(j\omega)=\frac{Q(j\omega)e^{-j\omega T_d}}{1-Q(j\omega)e^{-j\omega T_d}}\cdot L(j\omega) \qquad 3.6$$

In chapter 4 the filters will be designed and stability plots will be generated.

3.4 Robust repetitive control

Robust repetitive control makes use of multiple delays. The goal of robust repetitive control is to make the controller less sensitive for uncertainties in the period time. This is done by widening the peeks in the transfer function of the memory loop. In this way the sensitivity *around* the period frequencies is suppressed more and an error reduction still occurs, although the period frequency is not exactly as estimated.
There are different configurations possible. In figure 3.8 a general set-up of the memory loop M is given, containing three delays [4].

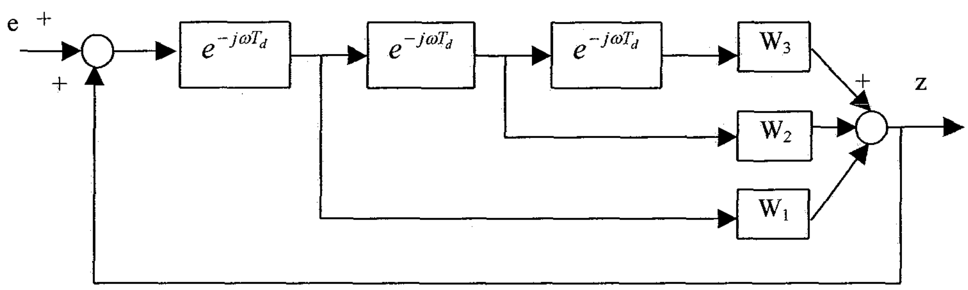

Figure 3.8, generalized repetitive controller

In the generalized multiple repetitive configuration, the low pass filter and the learning filter have been left out. For further implementation both filters should be placed back in the scheme. In this case however the idea behind the configuration can be explained with only the delays and the weighting factors.
The frequency response belonging to the generalized repetitive control with N delay loops is given by formula 3.7.

$$M(j\omega)=\frac{H(j\omega)}{1-H(j\omega)} \qquad H(j\omega)=\sum_{i=1}^{N}W_i e^{-j\omega i T_d} \qquad 3.7$$

As with repetitive control $M(j\omega)$ should still become infinite for $\omega = k2\pi/T_d$, $k=1, 2, 3,\ldots$. This means that $H(j\omega)$ should equal 1.
Given the fact that the pure delay equals one at $\omega = k2\pi/T_d$, an equation appears for the weighting filters:

$$H\left(\omega=\frac{k2\pi}{T_d}\right)=\sum_{i=1}^{N}W_i=1 \qquad 3.8$$

Steinbuch [5] proposed an algorithm to make the repetitive controller more robust with respect to uncertain period times. This is done by looking at the derivatives of $H(j\omega)$ with respect to the period time T_d. If the derivative of $H(j\omega)$ for $\omega = k2\pi/T_d$ is set to zero, the peeks of $M(j\omega)$ have zero slope at the period frequencies. This results in a wider top and base of the peeks. If the second derivative is set to zero too, the peeks get even wider. The more memory loops are used, the wider the base of the peeks.
The weighting factors that that belong to this robust algorithm can be calculated by formula 3.9 and 3.10.

$$\frac{\partial H(j\omega)}{\partial T_d} = \frac{\partial \sum_{i=1}^{N} W_i e^{-j\omega T_d}}{\partial T_d} = \sum_{i=1}^{N} -W_i ij\omega e^{-j\omega T_d} = 0 \longrightarrow \frac{\partial H(^{jk2\pi}/_{T_d})}{\partial T_d} = \sum_{i=1}^{N} W_i i = 0 \qquad 3.9$$

The same goes for higher order derivatives up to the N-1 th derivative.

$$\sum_{i=1}^{N} W_i i^{(Z-1)} = 0 \quad , for\ 1 \le Z \le N-1 \qquad 3.10$$

In figure 3.9 the magnitude frequency response of this robust repetitive controller is shown.

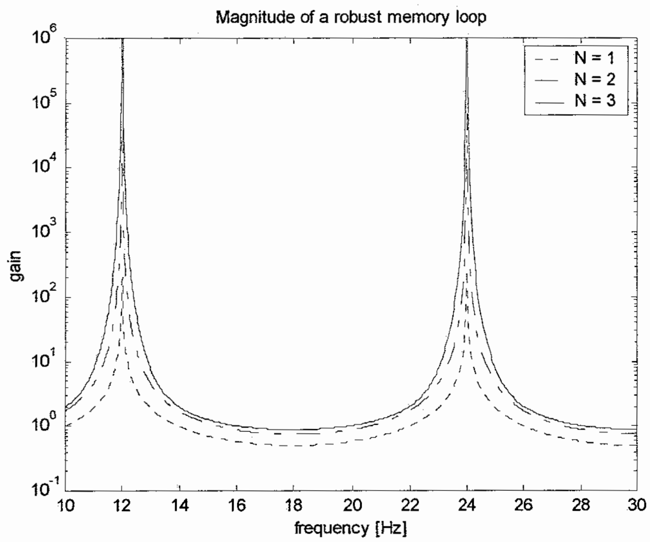

Figure 3.9, magnitude plot of memory loops with N the number of delays

A robust repetitive controller with N memory loops can be written by:

$$M(j\omega) = \frac{1-(1-e^{-j\omega T_d})^N}{(1-e^{-j\omega T_d})^N} \qquad 3.11$$

When formula 3.11 is written in expanded form, the parameters of the exponential terms are equal to the weighting factors.
As expected, the peeks get wider as the number of memory loops increase. Between the period frequencies, the amplitude of the magnitude frequency response increases with the number of loops.

Singh [6] proposed another configuration for robust repetitive control, which gives a smaller gain between the period frequencies. The scheme is given by figure 3.10.

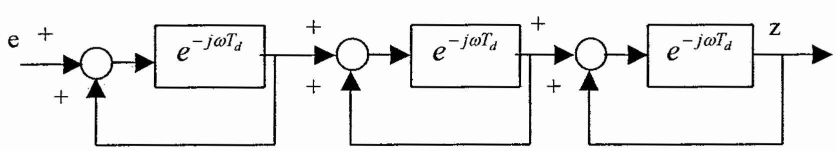

Figure 3.10, robust repetitive controller concept by Singh

The frequency response for the Singh robust repetitive controller is as follows:

$$M(j\omega) = \frac{(e^{-j\omega T_d})^N}{(1-e^{-j\omega T_d})^N} \qquad 3.12$$

The difference between this controller and that of Steinbuch is that the numerator of M is different. In figure 3.11 the controller of Steinbuch is compared to the controller Singh proposed.

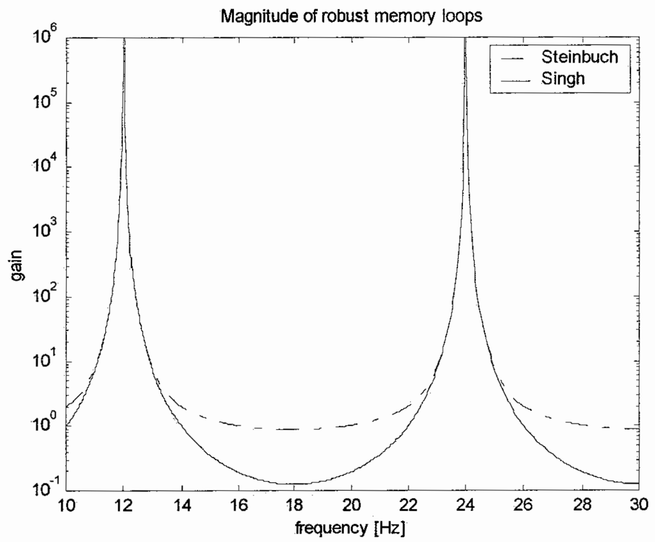

Figure 3.11, comparison between the Steinbuch and Singh configuration for N=3

One can see that the controller of Singh has a smaller gain between the period frequencies. If this will have any effect on the stability of the model shall be investigated in the next chapter.

4. Filter shaping

To guarantee stability of the (robust) repetitive controller, a learning filter and low pass filter are needed. In this chapter different filters are proposed to stabilize the system and optimise its performance.

4.1 Learning filter

The first filter that will be investigated is the learning filter L. As seen in paragraph 3.3 L should look like the inverse complementary sensitivity T^{-1}. In chapter 2 two inverse complementary sensitivities have been derived (phase one and two). For the learning filter, T^{-1} of phase one should be used. The reason for this is, that the phase two feedback controller already dealt with the dynamics of Dspace, so only the original T of phase one remains.
In many applications the inverse complementary sensitivity is unstable and non-proper and thus cannot be used as a filter. To solve this problem Tomizuka et al. [7] proposed a discrete approximation for T^{1} by using the Zero Phase Error Tracking Controller (zpetc) algorithm. The algorithm uses a discrete complementary sensitivity as input and returns a *stable* discrete inverse complementary sensitivity together with a pure delay.
In this study the L filter becomes $kT^{-1}(z)$ instead of $kT^{-1}(j\omega)$. The learning gain k is a parameter that has a default value of one. The optimal value for k has to be derived from experiments. The problems with pure delays will be solved in paragraph 4.3.
In figure 4.1 the Bode plots of the original complementary sensitivity and the approximation are given. The pure delay turns out to be three sample times when sampled with 25 kHz. In the phase plot, the phase caused by the delay has been taken into account.

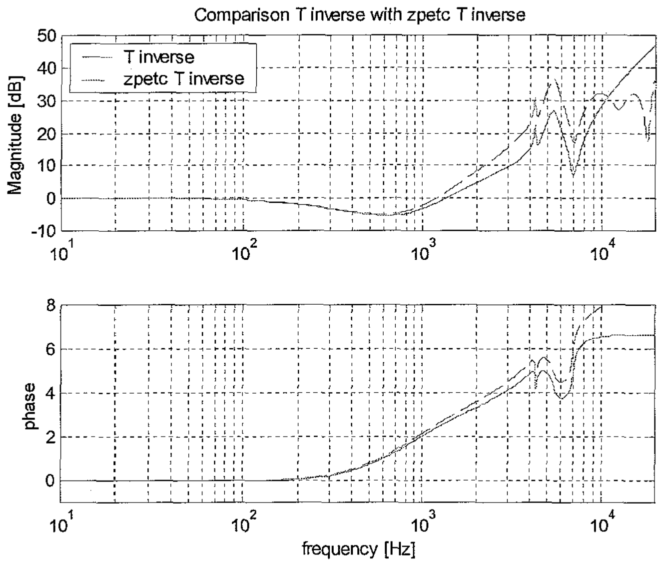

Figure 4.1, inverse complementary sensitivity, original versus zpetc

4.2 Low pass filter

The second filter that will be investigated is the low pass filter. There are several different low pass filters available that can be used as the low pass filter for the model. In this study three types are discussed: continuous time first order low pass filter, continuous time elliptic filter and the discrete time FIR filter.

The main difference between the filters is the phase shift. This phase shift could give stability problems, as will be shown later on in this chapter.

The first order continuous time low pass filter has the following transfer function:

$$Q(s) = \frac{1}{\frac{1}{\omega_c} s + 1} \qquad 4.1$$

In formula 4.1 ω_c is the cross-over frequency [*rad/s*]. The Bode plot for a first order low pass filter with a cross-over frequency of 10 *rad/s* is given by figure 4.2.

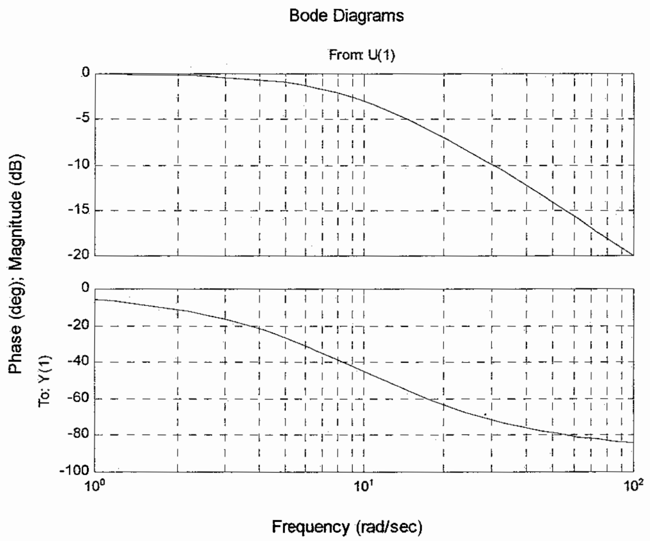

Figure 4.2, Bode plot of a continuous time first order low pass filter

The second filter is an elliptic filter. There are different parameters that must be specified before the filter can be generated. These parameters are the order of the filter, the ripple in the pass band (R_p [*dB*]), the cut-off frequency (ω_n [*rad/s*]) and the attenuation in the stop-band (R_s [*dB*]). These parameters, together with a sixth order continuous time elliptic filter, are shown in figure 4.3.

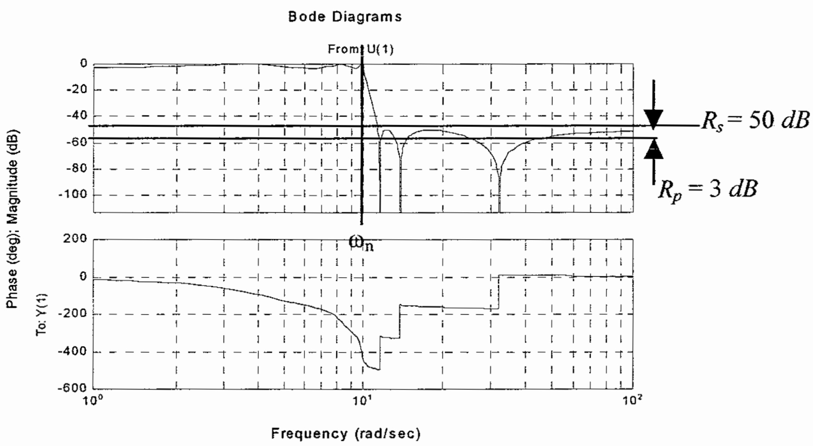

Figure 4.3, continuous time elliptic low pass filter

The transfer function of an n^{th} order continuous time elliptic filter is given by formula 4.2.

$$Q(s) = \frac{b(1)s^n + b(2)s^{n-1} + ... + b(n+1)}{s^n + a(2)s^{n-1} + ... + a(n+1)} \qquad 4.2$$

One of the differences between the elliptic filter and the low pass filter is that the phase of the elliptic filter has 'steps', while the first order low pass filter stays at –90 degrees.

The third filter is the discrete time FIR (finite impulse response) filter. The parameters that are needed for this filter are the order of the filter (n) and the cut-off frequency ($2\omega_n / f_s$, with f_s the sample frequency). The transfer function of an n^{th} order FIR filter is:

$$Q(z) = b(1) + b(2)z^{-1} + b(3)z^{-2} + ... + b(n+1)z^{-n} \qquad 4.3$$

The Bode plot for a 200^{th} order FIR filter with a cut-off frequency of 400 Hz and a 25 kHz sample rate is given in figure 4.4. The dashed line in the phase plot is the official delay found in literature [8].

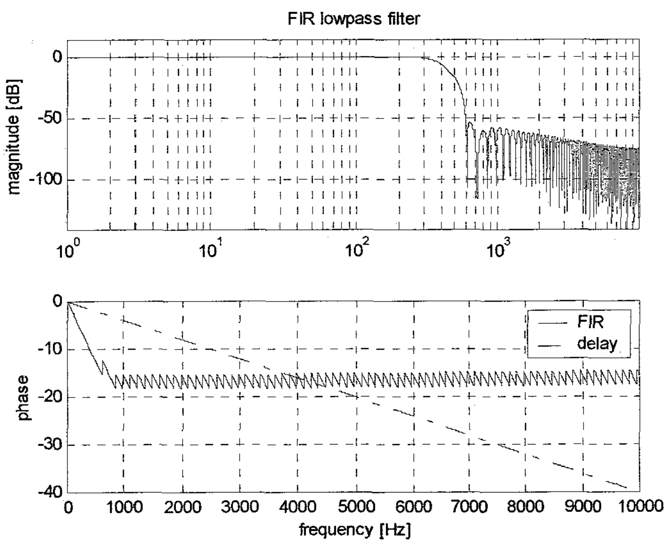

Figure 4.4, discrete time low pass FIR filter

The beauty of this last filter is that the phase shift is linear with the frequency. The consequence of this is that the FIR filter can be seen as a low pass filter without a phase shift but with a pure delay. For an even-order filter the delay is equal to half the order [8]. The saw tooth phase in figure 4.4 has probably been caused by uncertainties in the numerical calculations.
A possible drawback of this filter is that a relatively high order filter is needed to reach the desired cut-off frequency when the cut-off frequency is relatively small with respect to the sample frequency.
Nonetheless the fact that the FIR filter has linear phase shift is the reason why further implementation shall be done with this filter.

4.3 Dealing with the delays

Originally the memory loop contains one pure delay that is equal to the period time or, in discrete time, equal to N samples (= sample frequency divided by the period time). Because of the introduction of the stabilizing filters, some delay should be subtracted from the pure delay since they are already present in the stabilizing filters. The total delay time of the complete memory loop should be equal to T_d [s]. The pure

delay must thus be reduced by the delays from L and Q. The feedback loop inside the memory loop must have T_d delay too. To meet this demand, there has to be a delay in the feedback loop with a delay equal to the delay of the L filter.
When all this is implemented, the scheme of the memory loop looks like figure 4.5 and figure 4.6.

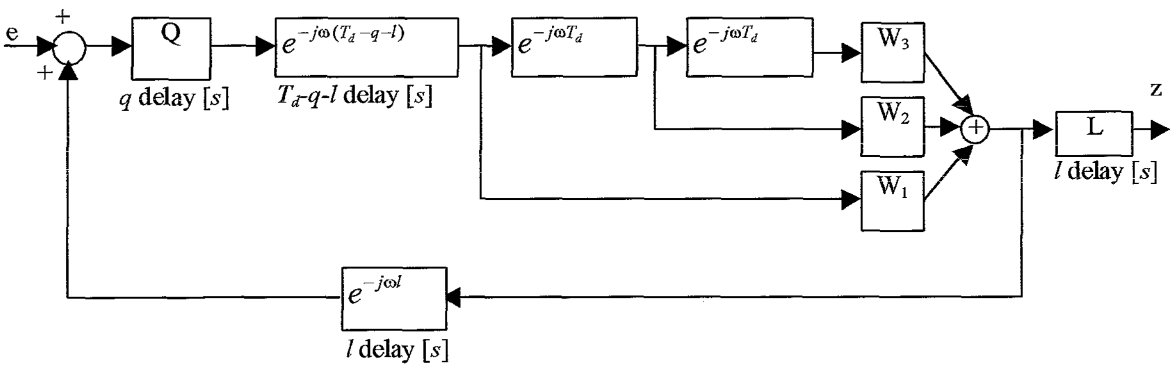

Figure 4.5, robust repetitive configuration with three memory loops, delays in the stabilizing filters are accounted for.

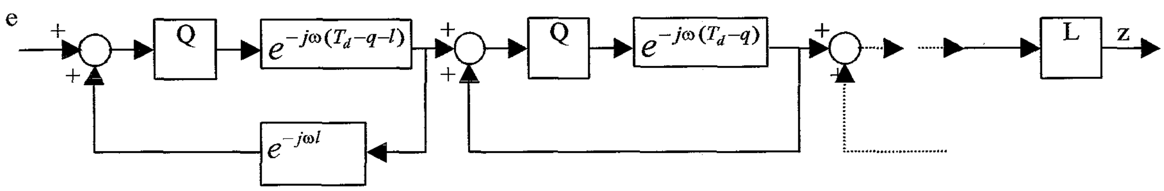

Figure 4.6, robust repetitive controller concept by Singh, delays in the stabilizing filters are accounted for

4.4 Sensitivity

In chapter 3 the sensitivity of a basic repetitive controller has been shown (figure 3.4). That sensitivity had not accounted for the dynamics of the stabilizing filters. In figure 4.7 the sensitivity of (robust) repetitive controllers with the configuration of Steinbuch has been plotted.

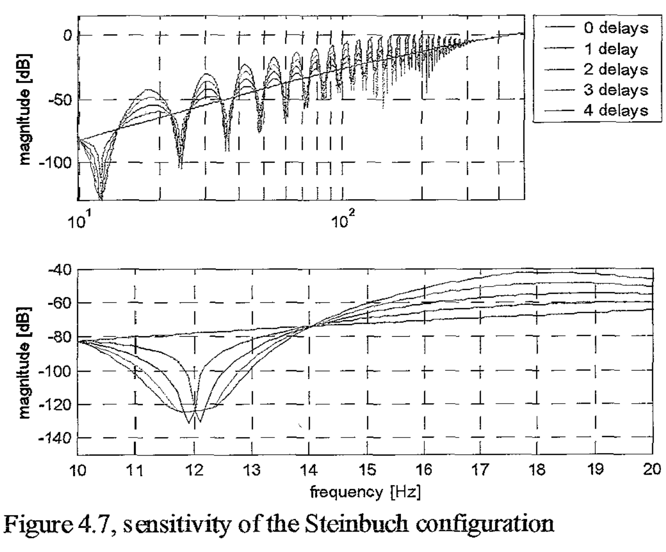

Figure 4.7, sensitivity of the Steinbuch configuration

Around the period frequencies a strange phenomenon occurs. The minima around the period frequency and its harmonics are not at those frequencies, but just before and after the period frequencies. The cause for this phenomenon is not known. As the number of memory loops increase, the phenomenon moves to higher frequencies, but occurs nonetheless. Besides the number of memory loops, also the order of the FIR filter influences the frequency band where the phenomenon occurs.
Looking at frequencies between the period frequencies, the gain increases with the increase of the number of pure delays

In figure 4.8 the sensitivity for the concept configuration of Singh is plotted.

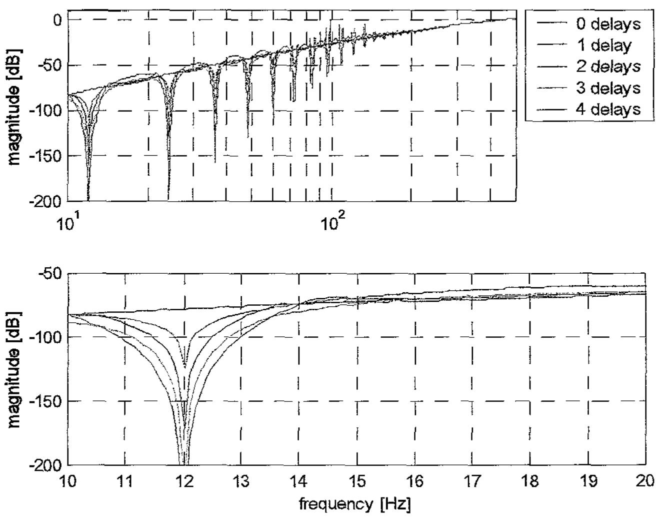

Figure 4.8, sensitivity of the Singh configuration

The sensitivity at the period frequencies is smaller than in the configuration of Steinbuch. The gain between the period frequencies is smaller too. This means that the errors with frequencies between the period frequencies are suppressed more with the Singh configuration than with the Steinbuch configuration.

In the figures above, the sensitivity is plotted for the case that the learning gain k is 1. What happens to the sensitivity when k is varied is shown in figure 4.9 and 4.10. The first plot shows the S for a repetitive controller, the second plot shows S including a three-delay memory loop, both controllers use the Steinbuch configuration.
When, in figure 4.9, the learning gain is increased, the plot gets sharp peeks between the period frequencies. If the system contains no noise of those frequencies perhaps this k value is better than $k = 1$. The suppression at the period frequencies is greater than with the default value of k.
When the learning gain is decreased, the gain between the period frequencies becomes smaller. The gain at the period frequencies is larger, so less suppression occurs.
For the case of three-delay robust repetitive controller the learning gain has another impact on the sensitivity plot. When k is increased more suppression at low period frequencies is seen and more gain at high period frequencies. For smaller learning gains the opposite occurs.
In test experiments some boundaries for k are found. For a repetitive controller the learning gain can have any value between 0 and 2. In case of a three-delay robust repetitive controller k can only be varied between 0.9 and 1.1. When other values are used, the system becomes unstable.
Due to the limited time available for the study, optimising the (robust) repetitive controller with respect to the learning gain is not further investigated.

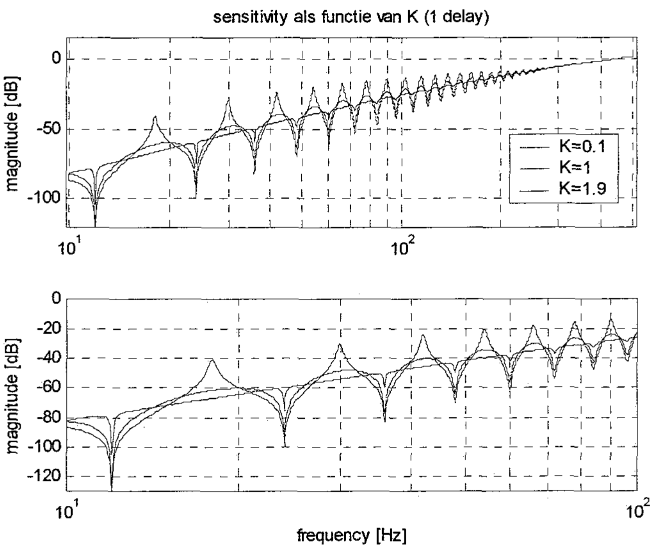

Figure 4.9, influence of learning gain k on the sensitivity of a 1 delay repetitive controller

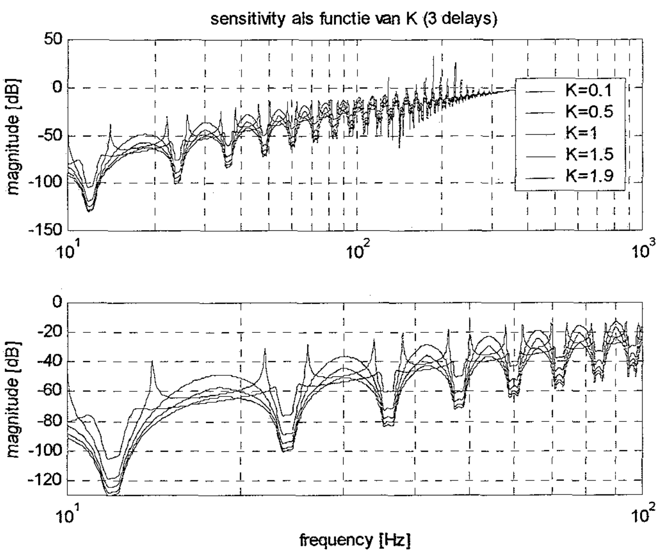

Figure 4.10, influence of learning gain k on the sensitivity of a 3 delay robust repetitive controller

4.5 Small gain theorem

To conclude this chapter the stability of (robust) repetitive controllers is investigated. This is done according to the small gain theorem.
Before the configurations of Steinbuch and Singh are investigated, the stability is tested with formula 3.5c with a repetitive controller (1 delay) without the additional extra delays. This is done for four cases: 1) no low pass filter, 2) a continuous time first order low pass filter, 3) an continuous time first order elliptic low pass filter and 4) a discreet 200^{th} order low pass FIR filter. The complementary sensitivity that has been used is obtained from the measurement of the phase two plant and controller.
In figure 4.11 the stability plots are presented. The figure is plotted in the complex plane. If the criterion goes outside the unity circle the amplitude of the criterion is larger than one and instability can occur.

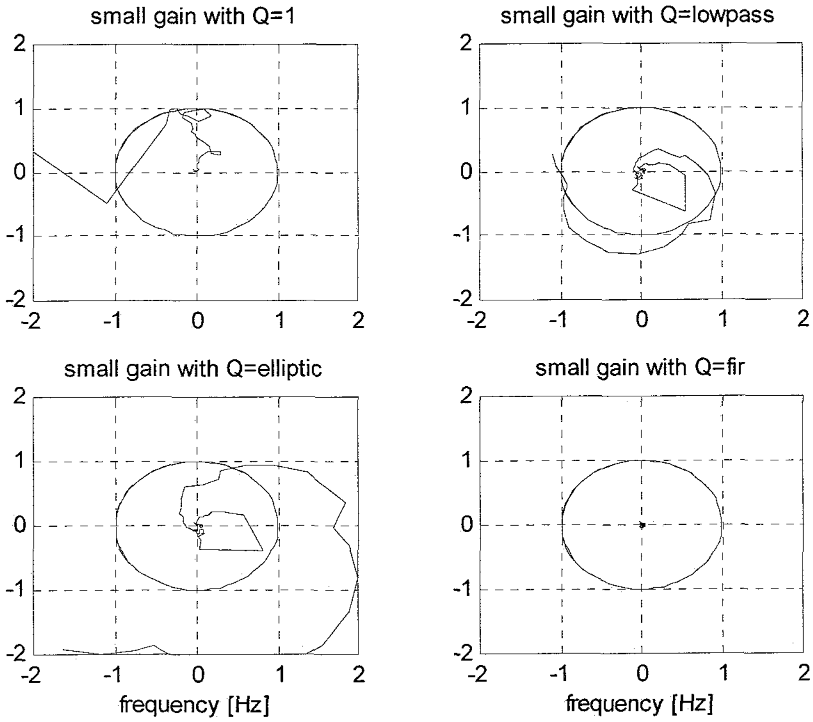

Figure 4.11, the stability criterion for the four cases

The only filter that stays inside the unity circle is the FIR filter. According to this analysis, when the other filters will be used, the system is not guaranteed to be stable.

Now the robust repetitive controller will be investigated. First the concept of Steinbuch is looked at, then the concept of Singh.
According to the model of Steinbuch, the memory loop with N delays has the following frequency response.

$$M = \frac{Q(W_1 + W_2 e^{-j\omega T_d} + \ldots + W_{N+1} e^{-j\omega n T_d})\, e^{-j\omega(T_d - q - l)}}{1 - Q(W_1 + W_2 e^{-j\omega T_d} + \ldots + W_{N+1} e^{-j\omega n T_d})\, e^{-j\omega(T_d - q)}} L = \frac{A e^{-j\omega(T_d - q - l)}}{1 - A e^{-j\omega(T_d - q)}} L \qquad 4.4$$

with $A = Q(W_1 + W_2 e^{-j\omega T_d} + \ldots + W_{N+1} e^{-j\omega n T_d})$ 4.4b

When M of formula 4.4 is filled in, in formula 3.3 and the sensitivity is transformed to small gain representation, the next expression appears.

$$S = \frac{1}{1+PC}(1 - A e^{-j\omega(T_d - q - l)})\left[\frac{1}{1 - A e^{-j\omega(T_d - q)}(1 - TLe^{-j\omega l})}\right] \qquad 4.5$$

and the stability criterion becomes

$$\left| A e^{-j\omega(T_d - q)}(1 - TLe^{-j\omega l}) \right| < 1 \qquad 4.6$$

In figure 4.12 the small gain criterion is plotted.

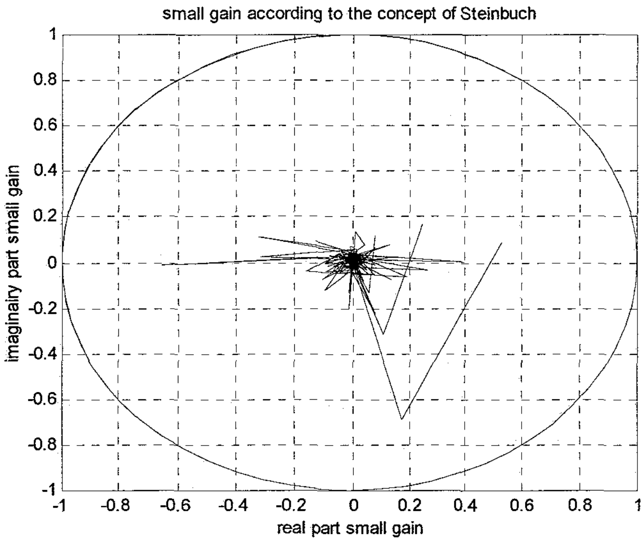

Figure 4.12, small gain with respect to the concept of Steinbuch

Although the plot isn't very clear, one can see that the model is stable up till the four delays plotted. The more delays are being used in the memory loop the closer the criterion approaches the unity circle. So there will be an upper bound to the number of delays that can be used in the memory loop.

The same procedure is done with the concept of Singh. The next formulas give the frequency responses of respectively: the memory loop, the sensitivity in small gain representation and the small gain criterion.

$$M = \frac{Qe^{-j\omega(T_d-q-l)}(Qe^{-j\omega(T_d-q)})^{N-1}}{(1-Qe^{-j\omega(T_d-q)})^{N}} L \qquad 4.7$$

$$S = \frac{1}{1+PC}(1-Qe^{-j\omega(T_d-q)})^{N}\left[\frac{1}{1-\left(1-(1-Qe^{-j\omega(T_d-q)})^{N}-TLQe^{-j\omega(T_d-q-l)}(Qe^{-j\omega(T_d-q)})^{N-1}\right)}\right] \qquad 4.8$$

$$\left|1-(1-Qe^{-j\omega(T_d-q)})^{N}-TLQe^{-j\omega(T_d-q-l)}(Qe^{-j\omega(T_d-q)})^{N-1}\right|<1 \qquad 4.9$$

In figure 4.13 the small gain criterion according to formula 4.9 is plotted.

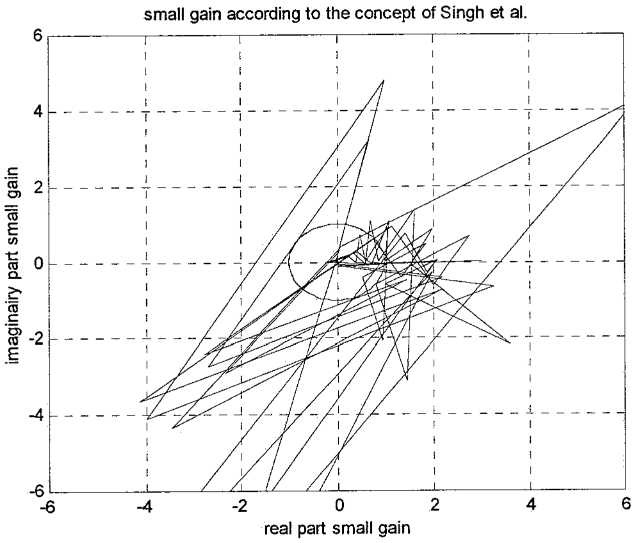

Figure 4.13, Small gain with respect to the concept of Singh et al.

As can be seen, the concept of Singh is always unstable, except for a one-delay memory loop, which has the same configuration as Steinbuch. Test simulations give the same result.
Simulations and experiments shall thus only be done with the (robust) repetitive controller configuration proposed by Steinbuch.

5. Simulations

The model of the (robust) repetitive controller is finished. The next step is to do simulations with the found configuration. Unfortunately there are still some problems with the design. These will be explained and solved first, after which the simulations are presented.

The first problem with the configuration is that the transient response of the reference signal is repeated by the memory loop. The peek in the error signal caused by the transient response gets smaller after each period and disappears after a while. Nonetheless in the beginning the peeks are larger than the specification (error smaller than +/- 0.1 μm) and thus not wanted.
To solve this problem, a switch is introduced. The memory loop is switched on after the transient response has disappeared. In this way, the memory loop does not have to deal with the transient response and the peeks do not appear.

When simulations are done with the period time of the reference signal equal to the period time in the delays (the ideal situation), a strange noise appears. The errors are larger when the period is exactly known, than when the period is not exactly known.
This problem is caused by the sample frequency. The sample time has to be precisely known. For example, a f_s of 25 kHz or 40 kHz is allowed, while sample frequencies between these values are not; 1/25e3 (4e-5) and 1/40e3 (2.5e-5) give precise numbers, while the other values are rounded at the seventeenth digit. Apparently the simulations are very sensitive for this.

After these problems are solved, the next Simulink scheme is found, given by figure 5.1.

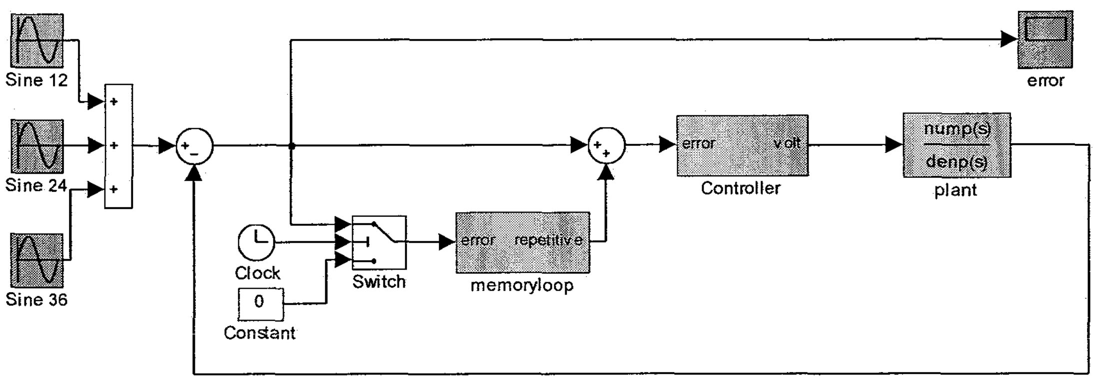

Figure 5.1, the Simulink scheme for a (robust) repetitive controller

The simulations that are done with Simulink are related uncertainties in the period time. The reference signal is kept the same, while the period time in the delays varies between 99% and 101% of the reference period time.
Figure 5.2 gives the results of the simulations, where the reference period time and the delay-period time both are 1/12 *s*. Subplot 1 gives the comparison between a simple feedback controller and the (robust) repetitive controllers (three lines at the x-axis). The second subplot zooms in at the (robust) repetitive controllers. All three lines look the same. This can be expected since the gains of the sensitivity at the period frequencies are equal for all three controllers.

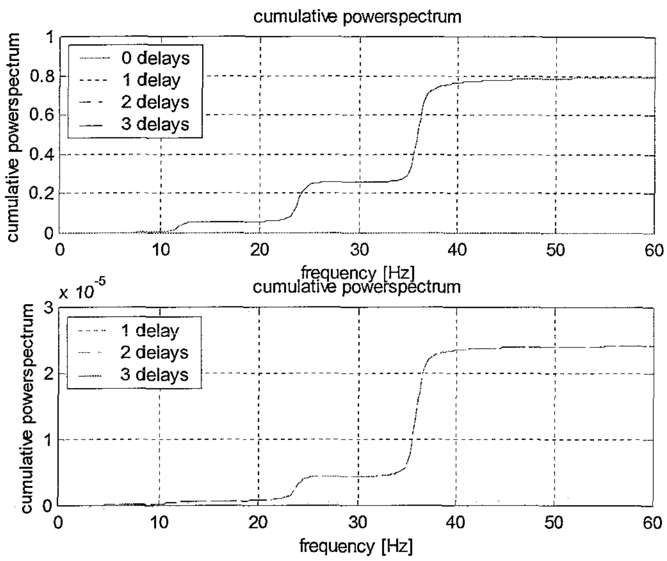

Figure 5.2, simulations where reference period time equals the delay time (1/12 s)

Figure 5.3 gives the results of simulations with the (robust) repetitive controllers when the delay time is varied. The results of the simulations with 12.0 Hz are at the x-axis; there too small to show.

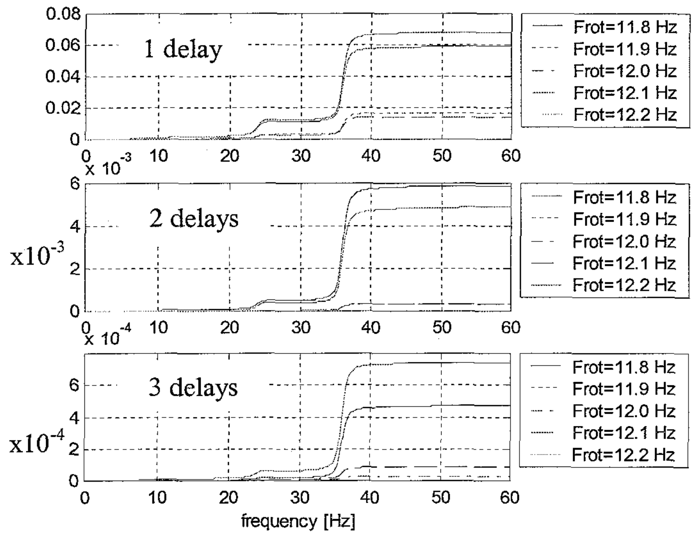

Figure 5.3, a) rep. cont. (1 delay), b) robust rep. cont.(2 delays), c) robust rep. cont. (3 delays)

Looking at the scaling of the y-axis, the robust repetitive controller with three delays is the least sensitive to uncertainties in the period time and returns the smallest error signals. The repetitive controller is the most sensitive, as expected.

Simulations give the same results as found in the calculations of the sensitivities and the theory. All seems to work as planned, so now experiments on the CD-player set-up can be done. The results of those experiments are presented in chapter 6.

6. Experiments

If measurements with the repetitive controller want to be done, the Simulink model has to be converted for real time implementation. This conversion is done by using Dspace.
The experiments that are presented in this chapter have been done with a sample frequency of 25 kHz, a 200th order low pass FIR filter and a learning gain of 1. While the values of these parameters are kept constant, the period time, the number of delays and the cut-off frequency of the FIR filter are varied.

Before the repetitive controller can be used, the period time of de CD-player has to be estimated first. This is done by using the errors measured with the different feedback controllers. After making cumulative power spectra of these errors, an estimation of the period time has been found. The 'steps' in the plot appear after every 12.7-12.8 Hz, so the period time is assumed to be around 12.75 Hz.
In an attempt to filter out the influence of local errors, the record length of the measurement is set to three seconds. In the hope to have the same track during each experiment, the starting position is located in the same area of the CD. If the track is the same each time, the error on the disk should also be the same and an accurate comparison between the different controllers can be done. Unfortunately the positioning isn't very accurate, since the radial arm is put in position by hand.
In figure 6.1 three experiments with a three-delay memory loop are shown. The settings of the controller are kept the same; only the starting points can differ, because of the uncertainty of the positioning.

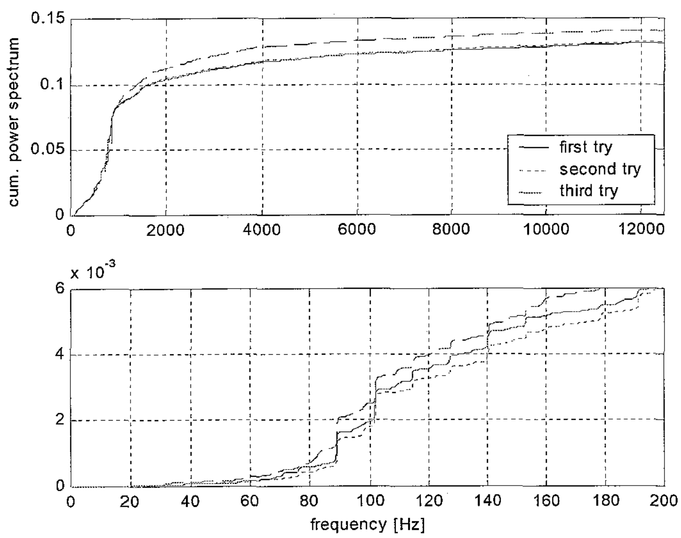

Figure 6.1, the influence of the starting position on the radial error

The most important conclusion from these experiments is, that the repetitive controller seems to work. The period frequencies up till 60 Hz have been filtered out almost completely.
From this experiment one can also conclude that *one* control setting can give different results. There is a difference of 0.01 in the different cumulative power spectra. If different experiments give results that are relatively close to one another, no accurate conclusions can be made.

The second experiment that has been done is with a period time of 12.75 Hz and a varying number of delays. In figure 6.2 the results are plotted.

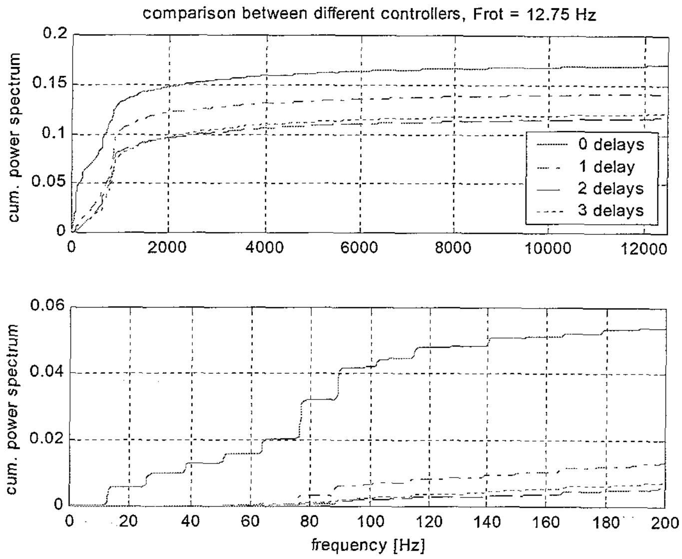

Figure 6.2, comparison between the error signals of the different controllers

The error signals decrease when the repetitive controllers are used. The difference between the errors with and without the repetitive controllers can especially be seen at the low frequencies (where the repetitive controller is the most active).
When the number of delays increases the power spectra get even smaller. A conclusion that can be drawn from that is that the estimated period frequency is not accurate, otherwise the three repetitive controllers should approximately have the same error signal.
In chapter 2, figure 2.6 a remark has been made about the errors of the phase one and two controllers. In figure 6.2 a 0-delay-error is presented that lays between the errors in figure 2.6. It could be possible that a feedback controller is more sensitive to the starting position than a repetitive controller and thereby produces more fluctuating errors. This is however not further investigated.

The next experiments that have been done are with various period times. In the figures 6.3-6.6, the results are presented. In the experiments the period time is varied between 99% and 101% in steps of a half percent. The cut-off frequency of the FIR filter is 120 Hz.

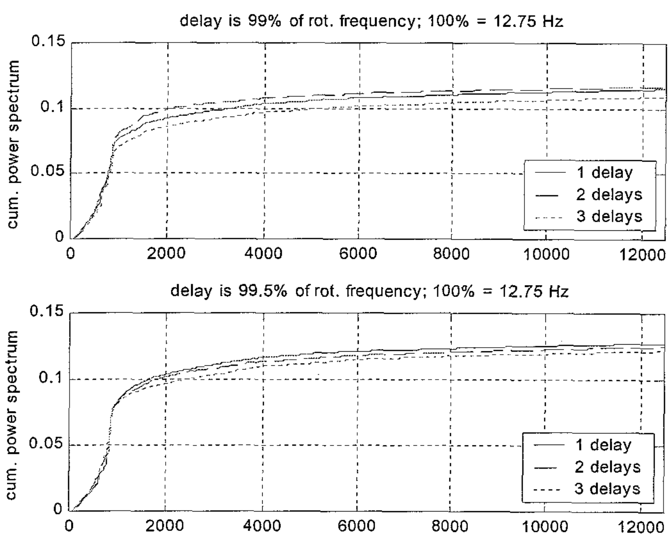

Figure 6.3, the total delay time is equal to 99% respectively 99.5% of the estimated period time

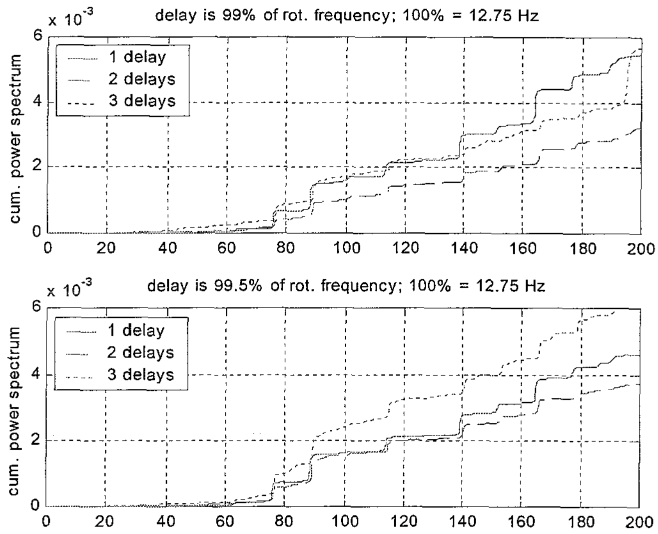

Figure 6.4, zoomed in on figure 6.3 from 0 Hz to 200 Hz

In figure 6.3 one can see that the final values of the cumulative power spectra are all approximately the same. This could mean that the real period time is between 99% and 99.5% of the estimated one, because, when looking at the sensitivity, the gain at the period frequencies is the same for all (robust) repetitive controllers.

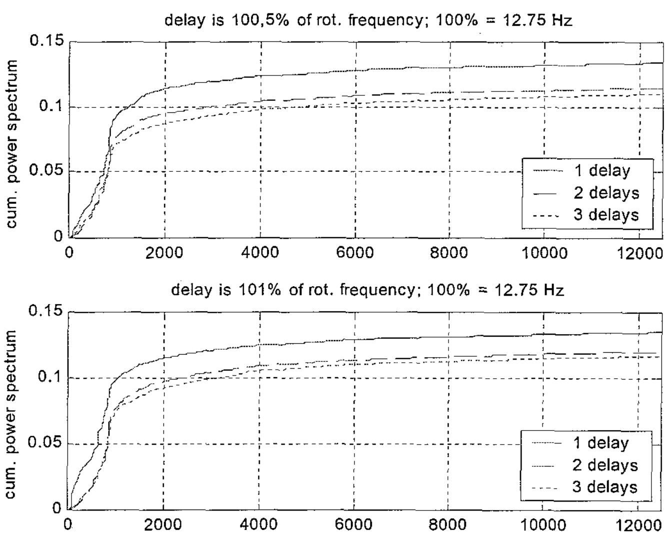

Figure 6.5, the total delay time is equal to 100.5% respectively 101% of the estimated period time

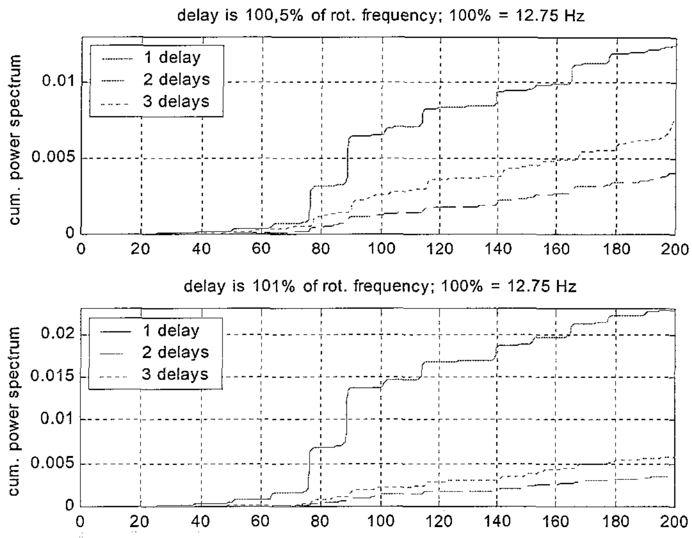

Figure 6.6, zoomed in on figure 6.5 from 0 Hz to 200 Hz

As the period frequency increases, the effect of the robust repetitive controller becomes visible. While the error of the repetitive controller with one delay increases, the robust repetitive controllers generate the same error signal.
Looking at low frequencies, it seems that the two-delay repetitive controller gives better results than the three-delay repetitive controller. This could be the case, but it can also be the result of the uncertainty of the begin position on the radial error. When the begin position can be determined more precisely, more precise conclusions can be drawn.
Up to around 60 Hz, the repetitive controllers filter out all the low frequency errors. The memory loop functions very well up to these frequencies. The expectation however is that the controllers suppresses the errors up to around 120 Hz.

To see the influence of variations in the cut-off frequency of the low pass FIR filter on the error signal, new experiments have been done. In figure 6.7 the results from experiments with different cut-off frequencies are shown.

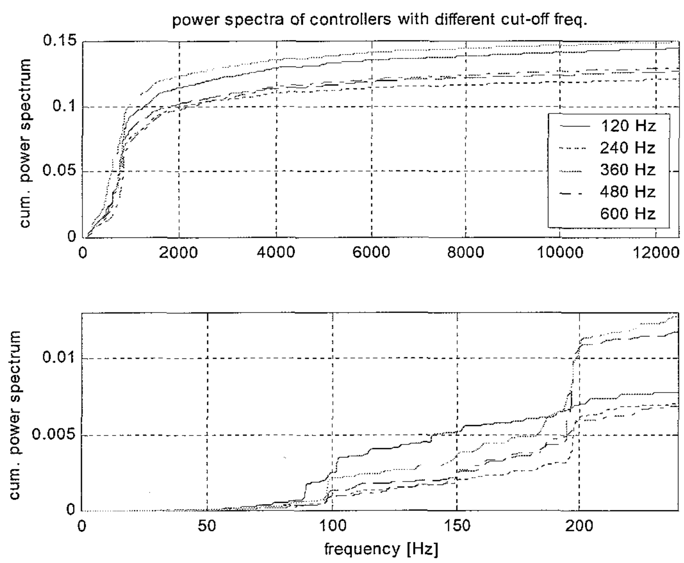

Figure 6.7, error signals from a robust repetitive controller with varying cut-off frequency

It appears that the cut-off frequency does not have much effect on the error signals, although slight more suppression occurs when the cut-off frequency is increased. The reason why the filter doesn't work as expected isn't known.
The reason why the 600 Hz error is larger than the others is possibly because the 600 Hz filter is close to instability. Experiments with higher cut-off frequencies were unstable.

Conclusions and recommendations

The subject of this report is repetitive control. Several steps have been taken, in order to understand and implement the controller. First of all, a simple feedback controller has been designed. With the controlled model the basic system is formed so the repetitive controller can be added.
Next, the theory behind memory loops, repetitive control and robust repetitive control has been studied. Two filters are introduced into the repetitive scheme, in order to guarantee stability. These filters have been designed and the repetitive scheme is adapted so that the whole controller satisfies the specifications again. With the adapted repetitive controller different simulations have been done, followed by experiments.

From the experiments, it can be concluded that the repetitive and robust repetitive controllers give promising results. According to simulations the error signal should be much smaller than is actually is, but then there has been no noise present in the simulations.
Low frequent noise, due to eccentricity of the disk and tracks and the wobbling of the spindle motor, is filtered out very well by the repetitive controllers. When perturbations in the period time are introduced, the robust repetitive controller shows its effectiveness.
The influence of the cut-off frequency of the low pass filter on the resulting error is not yet understood. There appears to be an optimal cut-off frequency, possibly a compromise between stability and the number of period frequencies that one wants to suppress. Perhaps it is just be the result of noise in the error signal. It is left for future studies to investigate this phenomenon.
A problem that occurs during experiments is that the radial arm cannot be positioned accurately. This way each experiment could give another error signal and comparison between experiments is more difficult. If more precise measurements are needed, this problem should be solved.

Besides the above conclusions and recommendations, there are some more remarks, summarized by the following points.

- In the experiments a sample frequency of 25 kHz has been used and the period time is around the 12.75 Hz. This means that when a single delay memory loop is used the memory loop needs a capacity of 1961 places to store the information of the last period. When a robust version of the repetitive controller is used, the storage capacity should be even bigger.
  To reduce the necessary capacity, down sampling in the memory loop is advised. In this way, the controller becomes more interesting for commercial applications.
- Repetitive control uses the fact that the period time has a constant value. If an adaptive repetitive control algorithm can be derived to estimate the period time / rotational frequency real time, the need for a precise estimation of the period time will become absolute. Besides that, the repetitive controller will be able to deal with (slow) changes in period time and the diversity in applications will increase.
- When the error of the repetitive controller becomes too large, the radial arm flips out and cannot be placed back on a track. The reason for this is that the memory loop fills itself with extreme errors. It then injects the signal back into the system one period later, so a wrong error is given to the feedback controller and tracking becomes very difficult.
  This problem can be overcome by resetting the memory loop when such an error signal occurs. The resetting should take place when the period that an error signal has large values, has crossed some predefined time span. Future studies should investigate the different parameters that are involved.
- The repetitive control concept of Singh turns out to be unstable. Further studies could investigate the concept and make adjustments so that stability is guaranteed.

References

[1] Jansens J., "Characterization of optical discs", DCT 2001-14, Eindhoven University of Technology, 2001

[2] Vd Molengraft M.J., "Disturbance cancellation in Compact Disc Applications", DCT 2001-61, Eindhoven University of Technology, 2001

[3] Kuijpers R., "Single period Learning for radial tracking of a CD player", DCT 2001-62, Eindhoven University of Technology, 2001

[4] De Hoog T.J., "Stability and performance of memory loop filtered control systems", PATO course, Delft University of Technology, 1997

[5] Steinbuch M., "Repetitive control for systems with uncertain period-time, with application to a compact disk drive", it Proc. 1st IFAC conference on Mechatronic Systems, 18-20 September 2000, Darmstadt, pp 409-414.

[6] Personal communication with T. Singh, 2001

[7] Tomizuka M., "Zero Phase Error Tracking Algorithm for digital Control", Trans. of ASME Journal of Dynamic Systems, Measurement and Control, Vol. 109, March 1987, pp 65-68

[8] "Programs for Digital Signal Processing", IEEE Acoustics, Speech and Signal Processing Society, New York: IEEE Press, 1979